DE- AI09-00SR22188 JOURNAL ARTICLE 2015 15-07-R

Final Report

Watershed modeling at the Savannah River Site

USFS Agreement Number 10-CS-11083601-002

12/1/2013 – 12/1/2014

Prepared by:

Kellie Vache

Oregon State University

Prepared for

USDA Forest Service Savannah River

P.O. Box 700

New Ellenton, SC 29809

The overall goal of the work was the development of a watershed scale model of hydrological function for application to the US Department of Energy's (DOE) Savannah River Site (SRS). The primary outcomes is a grid based hydrological modeling system the captures near surface runoff as well as groundwater recharge and contributions of groundwater to streams. The model includes a physically-based algorithm to capture both evaporation and transpiration from forestland. In addition, the model includes a tracer-based approach for estimating modeled residence time distributions for any location within system. This capacity has been included as a means to more fully characterize the dynamics of water storage and release in this region where groundwater flow is a large component of stream discharge.

The model has been applied at a variety of scales within SRS, including a set of 3 small, intensely gauged watersheds, the larger Upper Fourmile watershed, the entire Fourmile watershed, and more recently, the entire set of watersheds making up the majority of the SRS landscape. Application across this larger landscape will provide the basis for evaluating impacts on water quantity and water quality of the intensive pine production for biofuel feedstock that the overall study (both field and modeling components) is exploring.

The work developed under this project includes a modeling framework, and a set of models using the developed framework. This report outlines key products, and focuses on the development of the model at the smaller, gauged watersheds. A key outcome involves the development of peer-reviewed literature. The first paper, tentatively titled "Evaluating hydrological response of a groundwater dominated forested catchment in the Upper Coastal Plain of South Carolina" is currently under development and will focus on the development and application of the model, using field data collected at the smaller watersheds.

Introduction

The catchment modeling has been developed to explicitly capture water balance relationships in the three study watersheds, referred to as watersheds R, B, and C. The initial component of the work has been the development of a modeling tool that

1. makes use of the data available at the site, as both input and validation
2. is consistent with hydrological processes in the region
3. is sensitive to management strategies associated with the forestlands

This report documents the development of the model, outlining both key input datasets and model application, calibration and initial validation. The models for each of the 3 study watersheds successfully captures key elements of the water balance and the evaluation and verification process will continue as new site data becomes available and as we refine the conceptual model of catchment hydrologic function.

The modeling process, outlined here, started with the development of conceptual model, proceeded to the development of a numerical model designed to capture key hydrological features of the catchment, and then to calibration of the numerical model, using the R catchment as the initial location for development. We then used the developed structure and calibration to look at how well it functioned in different places (B and C watersheds) and at different times (in this case, a much wetter period, approximately 1 year after the calibration period). A direct transfer of parameters from the R watershed to B and C appears to acceptably capture the spatial distribution of water, though simulated stream discharge was not as high as observations suggest. To more fully evaluate this difference, we developed monte carlo simulations, varying model parameters over acceptable ranges, running the model multiple times, and looking for parameter sets that more fully captured the measured discharge. Results of the monte carlo simulation indicated a set of more plausible parameters, although we are in the process of re-evaluating the recharge model to more fully accommodate the recently updated conceptual model, based on interpretation of the continually developing observational data base.

The report is organized in 3 parts. Part 1 outlines the model, with particular emphasis on the evapotranspiration and energy balance components. These elements of the model have been recently added and represent a key connection between hydrological process and management. Part 2 includes an outline of the initial model calibration, and part 3 is comprised of a simple validation exercise, which led us to the monte carlo uncertainty procedure to identify potential structural inefficiencies in the model.

Part 1. Model Description

Lateral subsurface flows and groundwater

We employ a spatially-distributed catchment model that builds upon work outlined in Vaché and McDonnell (2006) The shallow subsurface flow routines follow from Wigmosta et al. (1994). This gridded scheme was selected as the basis for the model because it provides an explicit mechanism to incorporate transient subsurface flows and the gradients that play an important role in driving lateral flow and aging in the region. The model equations defining the near surface mass balances are fully documented in Vaché and McDonnell (2006), however the groundwater model which comprises the bulk of the discussion here has been recently added to the framework.

The development of the groundwater model began with an understanding of what the model was designed to capture; potential groundwater storages and fluxes in steep volcanic terrains and across relatively small watersheds. We implemented an approach similar in scope to the subsurface flow, depending on Dupuit-Forchheimer assumptions to define the groundwater system in 2 dimensions, and capturing that system with a simple mass balance approach using Darcy's law to define downslope groundwater fluxes.

The volume of water within the saturated zone of each reservoir is accounted for as:

$$\frac{dV_s}{dt} = R + q_{in} - q_{out} - K_d \qquad (1)$$

where V_s is the specific volume of water in each reservoir (m), t is current time (days), R is the groundwater recharge, q_{in} and q_{out} are the lateral fluxes into and out of the volume, and K_d is a loss rate from the base of the modeled volume.

q_{in} and q_{out} are defined as

$$q_{in} = \sum_{k=0}^{k<9} -K_k \frac{dh_k}{dx} \quad \text{for } \frac{dh_k}{dx} > 0 \qquad (2)$$

$$q_{out} = \sum_{k=0}^{k<9} -K_k \frac{dh_k}{dx} \quad \text{for } \frac{dh_k}{dx} < 0 \qquad (3)$$

Where K represents the saturated hydraulic conductivity, $\frac{dh}{dx}$ is the gradient between grid cells, defined based upon the deeper groundwater surface, and k is an index for each of the neighboring grid cells.

Evapotranspiration modeling and the influence of landuse management

A primary goal of the project is to develop techniques to allow for clearer understanding and predictive capability regarding the influence of vegetation and management on hydrological and biogeochemical cycles. Evapotranspiration (ET) is a key link between the water and energy cycles and is also significantly influenced by properties of both soils and vegetation. As such, it represents a key feature of the system that is being characterized by the project. The modeling of ET is a well-established field, with a range of potential options. Our incorporation of ET relies primarily on well-established literature reviews of the subject and is designed to insure that we capture the appropriate level of detail required to approach the overall project questions.

Potential versus reference ET

Potential ET is generally characterized as the amount of water that would be evaporated from an extensive free water surface under current meteorological conditions. Reference crop ET is the rate of evaporation from a well watered crop with some specific set of physical parameters. A commonly used reference crop is an idealized grass with a fixed height of 0.12 m, and albedo of 0.23, and a surface resistance of 69 s/m (Shuttleworth, 1993). Reference crop ET estimates can be modified to capture the reference ET from other crops through linear modifications using 'crop coefficients'.

Reference Crop versus Surface-dependent ET

Federer et al., (1996) compare a number of ET methods, distinguishing reference crop ET methods from a set of more sophisticated approaches that capture the influence of varying cover types directly. Surface-dependent models include directly both aerodynamic and surface resistances that characterize individual vegetation types. No assumptions regarding the particular surfaces are built into the models. They included Priestly-Taylor (P-T), Penman-Monteith (P-M), and Shuttleworth-Wallace (S-W) approaches in the evaluation of surface independent models. Preistley-Taylor is surface independent in that it accommodates surface resistance, as albedo. P-W depends on albedo and also aerodynamic resistance. The S-W type approach separates transpiration from soil evaporation, using surface resistance terms in addition to albedo and aerodynamic resistances. A common strategy used in either type of model is to use weather variables to determine to potential ET given an unlimited supply of water, but to additionally provide an estimate of actual ET given available soil water and perhaps root density distributions.

Models that are designed to provide predictive capacity related to vegetation change have to accommodate the influence of those changes on ET, and surface-dependent models are the appropriate choice. These models typically are based on the P-M equation which assumes the vegetation cover can be considered a single 'big leaf' which intercepts most of the available radiant energy. Shuttleworth (1993) defined it as:

$$E = \frac{1}{\lambda}\left[\frac{\Delta A + \rho_a c_p D / r_a}{\Delta + \gamma(1 + r_s/r_a)}\right] \qquad (4)$$

Where E is the evaporation rate in mm/d, λ is the latent heat of vaporization (MJ/kg), Δ is the gradient of the saturated vapor pressure (kPa/C), A is the available energy (MJ/m2/day), ρ_a is the density of air (kg/m3), c_p is the specific heat of moist air (1.013 kJ/kg/C) , D is the vapor pressure deficit (kPa) at the height Z for which r_a is calculated, r_a is the aerodynamic resistance (s/m), r_s is the surface (or stomatal) resistance (s/m), and γ is the psychrometric constant (kPa/C). It is also worth noting that the equation can capture both evaporation from wet canopy surfaces and transpiration when the canopy is dry by simply setting the surface resistance term to 0 during those periods. This can typically be accomplished when using the model as part of a running water balance that explicitly includes vegetation, interception, and soil water storage

The clearest differences between the surface-dependent models have to do with the assumptions made regarding r_a and r_s. The S-W type approaches further distinguish themselves by relaxing the P-M assumption that the vegetation is continuous and can be treated as a 'big leaf'. In areas where the canopy can be expected to change over time and space, S-W type approaches are preferred (Zhou et al., 1996). While more complicated, these models can provide estimates of wet and dry canopy evaporation as well as bare soil evaporation, and this distinction may be of significance when running distributed hydrological models that are designed to capture the influence of vegetation management strategies such as the short rotation biofuel harvests being evaluated at SRS.

There are three primary forest traits that the modeling is required to address from the standpoint of ET. The first is to capture variations ET rates across space and time as a function of diurnal, seasonal, and annual changes in the meteorological conditions that are captured at the site. The second is to capture variation of ET as a function of different vegetation types, different canopy layers, variable canopy density and changes associated with LAI seasonally and with vegetation age. The third is the capacity to estimate ET from bare soils, which will frequently exist given potential forest management strategies. Accommodating these factors begins with P-M, but does require the relaxation of the 'big-leaf' approach. Our formulation is based upon existing approaches and is similar to the S-W type approach outlined by Wigmosta et al. (1994), including the potential to simulate both overstory and understory canopies. The understory will likely not be important at SRS, but was included to provide additional flexibility for applications to different forested sites.

There are 5 primary components of the approach.

(1) The development of the energy budget,
(2) Canopy storage estimates
(3) Evaporation from canopy surfaces or soils through transpiration using P-M,
(4) Canopy and aerodynamic resistances.
(5) Evaporation from bare soils,

The energy budget

The shortwave and longwave energy budgets are developed following directly from Wigmosta et al. (1994) with separate budgets for each canopy layer and the ground surface. The key parameters in the energy budgets are projected LAI, fractional ground cover (F), and a reflectance coefficient to capture back reflection from the understory. The amount of shortwave radiation transmitted through each canopy layer is captured with a Beer's law relationship and the fractional cover is used to capture the sum of attenuated incoming shortwave and direct shortwave for the open fraction of the ground surface.

Incoming shortwave radiation, air temperature, dew point, and vapor pressure are provided to the model on subdaily timesteps, and relative humidity, saturated vapor pressure, and the vapor pressure deficit are estimated directly. Incoming downward longwave is estimated based on Shuttleworth (1993).

Canopy storage

Maximum canopy storage for both over and understories are estimated following Wigmosta et al. (1994) as:

$$I=10^{-4}LAI*F \quad (5)$$

Where F is the fraction of the ground surface covered by the overstory. It is set to 1 for the understory, when it exists and understory is included in the radiation balance. Through fall is generated anytime the amount of water in the canopy is larger than I.

Evapotranspiration

Evapotranspiration is separated into evaporation from wet canopy surfaces and soils, and transpiration through vegetation. Wet surface evaporation is calculated from (1) assuming no surface resistance, setting r_S set to zero. The model then calculates transpiration, with the stepwise approach accommodating both evaporation and transpiration within single timesteps (Wigmosta, et al., 1994).

Resistance Terms

Canopy resistance is typically influenced by LAI and meteorological conditions, expressed in the form

$$r_{s}=\frac{r_{s\,min}}{LAI_{e}f(X_{i})} \qquad (6)$$

Where R_{smin} is a minimum canopy resistance, LAI_e is the effective LAU, X_i represents the environmental variables on which R_s depends and f is a stress function that depends upon environmental conditions. We define R_{sj} based on four limiting factors related to air temperature, VPD, PAR and soil moisture. Definitions of each can be found in Wigmosta et al. (1994).

Aerodynamic resistance is used to control the rate of vapor transfer away from the ground and is inversely proportional to both wind speed and vegetation height. A variety of mechanisms have been proposed to capture aerodynamic resistance in P-M based models, and we make use of one of the more straightforward variations, proposed by Shuttleworth (1993):

$$r_{a}=\frac{ln[(z_{m}-d)/z_{om}]ln[(z_{e}-d)/z_{ov}]}{0.41^{2}(U_{z})} \qquad (7)$$

Where z_u and z_e are the heights of the wind speed and humidity measurements, U_z is the windspeed and z_{om} and z_{ov} are assumed to be $0.123h_c$ and $0.0123h_c$ respectively where h_c is the mean height of the canopy. D is assumed to be $0.67h_c$. Zhou et al. (2006) outline a somewhat more complex version to explicitly account for the aerodynamic resistance of both soil to canopy and canopy to reference height, as defined by Shuttleworth and Gurney (1990), and comparisons against this more sophisticated version are warranted.

Bare Soil Evaporation

Soil evaporation is calculated by replacing the surface resistance term in (1) with values that are appropriate for different soil types (Shuttleworth and Wallace, 1985). A number of soil moisture or texture dependent mechanisms have been proposed including:

$$r_{s}^{s}=\tau l/(pD_{v}) \qquad (8)$$

Where l is the depth of the upper layer, p is the porosity, τ is the tortuosity, and D_v is the molecular diffusion coefficient for water vapor. Typical applications appear to simplify the issue significantly, using constant values for the soil surface resistance. Zhou et al. (2006) note that it is often not possible to properly parameterize such models, and that both Shuttleworth and Wallace (1985) and Federer et al. (1996) used a value of 500s/m as reasonable based on available literature.

We have also implemented the soil evaporation model proposed by Wigmosta et al. (1994), but the simpler empirical approach proposed by Shuttleworth and Wallace (1985) appears to produce reasonable results. A more complete comparison of the two methods is warranted.

Part II. Calibration and evaluation of results

ET Modeling Example Results

The following are a set of exemplary model outputs that relate only to some of the key features that are captured in the ET and radiation balance components of the model. While there is work remaining to finish parameterization and verification of the model, the results are plausible and provide a mechanism to evaluate changes in ET as a function of meteorological conditions, canopy density, and LAI. This appears to be an appropriate level of complexity given the dimensions of the problem, and the immediate need is to more fully evaluate the model across a range of canopy conditions.

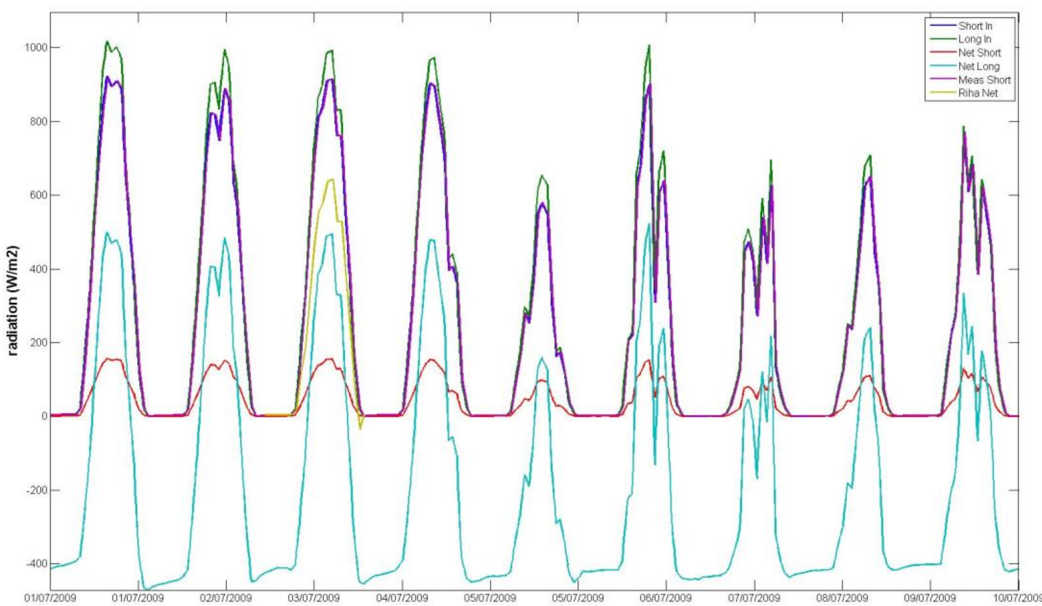

Figure 1. A time series figuring outlining key features of the radiation balance during an arbitrary 10 day period in the summer of 2009. These results assume a fully closed canopy. ‘Short In’ is the amount of incoming solar radiation reported as model output. For comparison, ‘Meas Short’ is a plot of the incoming shortwave reported as model output. They should be essentially the same, and differences are due to interpolation. ‘Long In’ is the estimated incoming longwave radiation. ‘Net Short’ and ‘Net Long’ are estimated values of the long and shortwave that is available for ET calculations (A in equation 1). The sum of these two values should be approximately equivalent to the ‘Riha Net’ timeseries – the Penman-based net radiation as calculated by Riha and others and included in the MET_DAT_CALC_@M_DLST.xls tritium ET calculation spreadsheet. The calculations are somewhat different, and some divergence is to be expected.

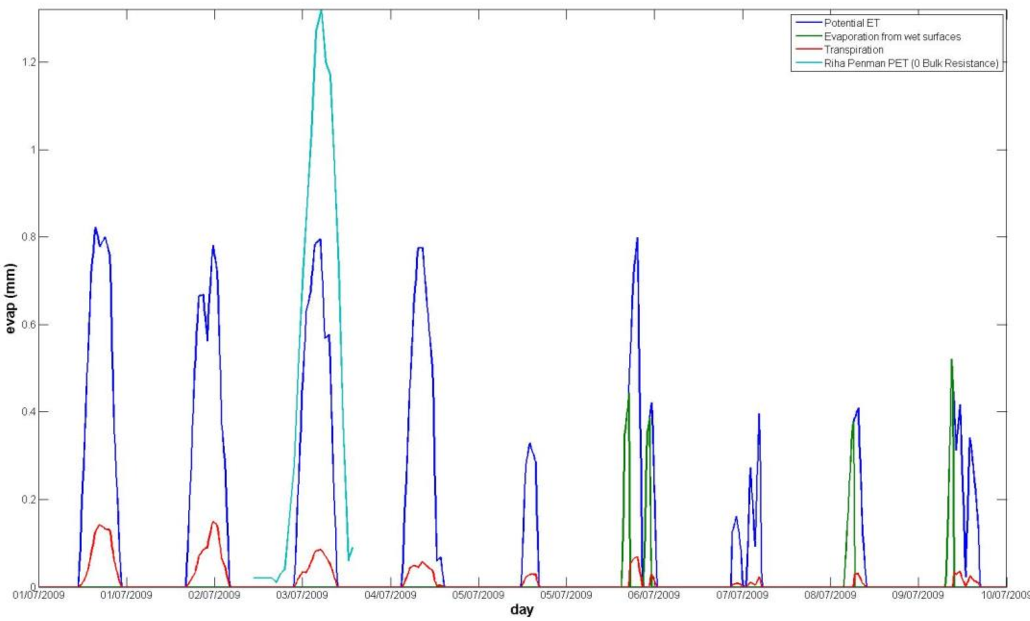

Figure 2. A set of key rates related to the ET modeling. ‘Potential ET’ is the simulated PET (mm/hr). It is compared against the ‘Riha Penman PET’ calculation for 1 of the days. The primary difference between the 2 estimates of PET is that the Riha calculations assume no bulk resistance, and should therefore be somewhat higher, as is demonstrated in the figure. The output also includes evaporation from wet surfaces and transpiration. Note that wet surface evaporation should be 0 except after rainfall.

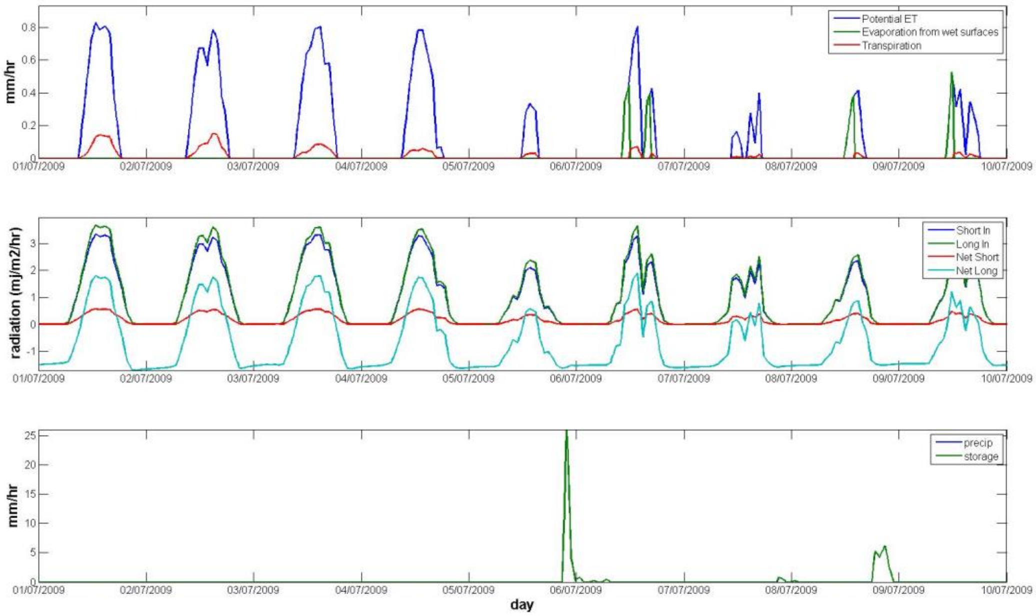

Figure 3. Time series values comparing elements of both figure 1 and figure 2. Precipitation and throughfall (labeled 'storage' in the figure) are also included and the units for the radiation balance have been converted to metric. Note that the precipitation event on the evening of the July 6 wetted canopy surfaces, allowing for the evaporation that occurred on July 7.

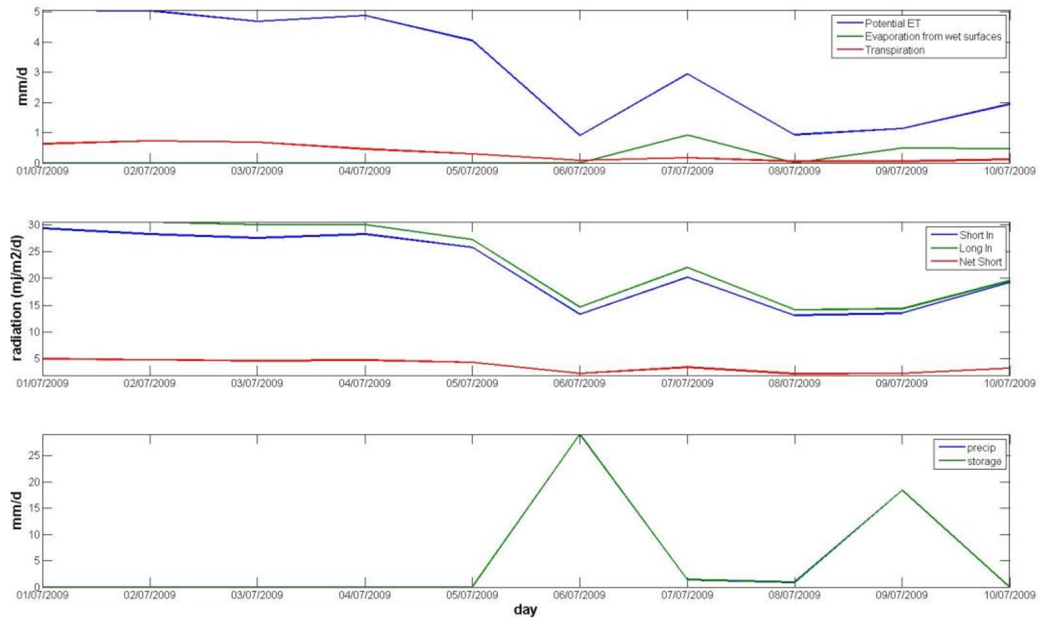

Figure 4. Daily summaries of figure 3. The information provided in the figure is equivalent to that in figure 3, but represents a coarser daily view of the radiation balance and ET calculations. This daily summary timeseries may be appropriate in the manuscript.

Part II Runoff modeling

Runoff modeling is focused on capturing measured hydrographs at the 3 sub watersheds, using available climate data. The focus has been on hourly simulations. Overall, the model appears to capture the spatial patterns of soil moisture and the general directions of groundwater flow. With more complete incorporation of the developing conceptual model, we anticipate that simulated flow dynamics will continue to improve.

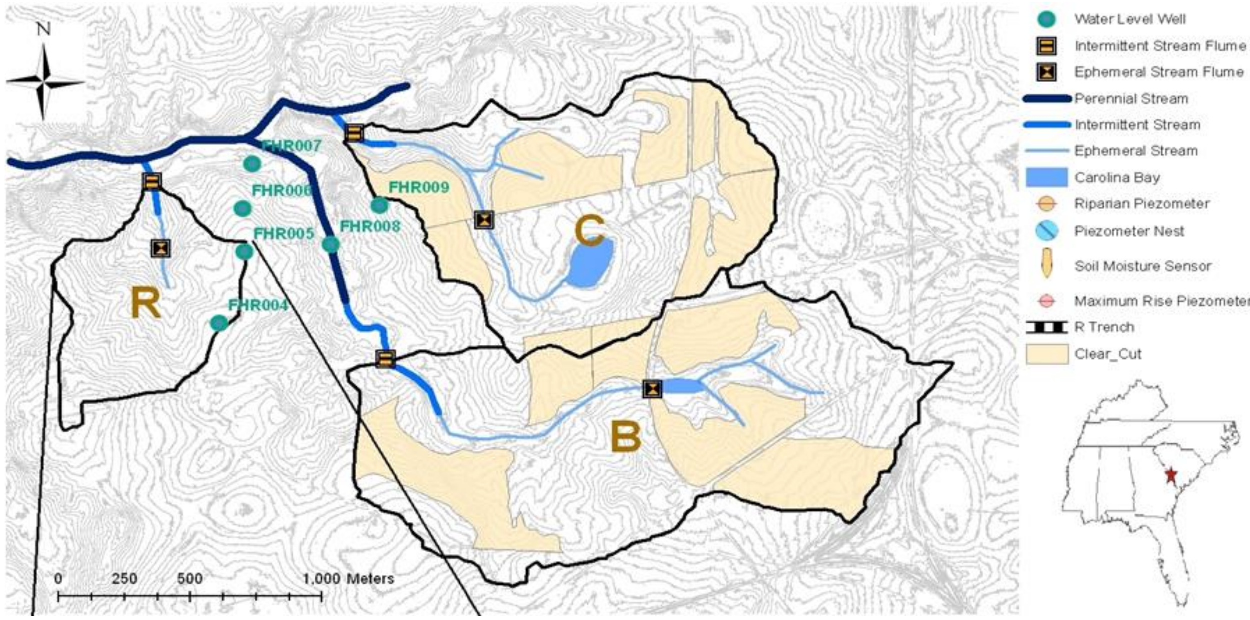

Figure 5. A site map outlining the locations of the R, B and C watersheds in SRS.

Calibrations at the R watershed

A key hydrologic feature of the site relates to the spatial patterns of soil moisture and groundwater, and how these spatial patterns interact with the vegetation and meteorology to produce runoff. One of the key observations at the site has been that the appearance of observed runoff is modulated by seasonal variation in deeper groundwater dynamics. During wet years, the area of intersection between groundwater and surface water increases, and along with it, the measured stream discharge, both in amount and extent, also increase. Figures 6-8 outline these spatial patterns for a wetter period of time. The evaluation of these spatial patterns and how the correspond to other observable quantities will continue with refinement of the conceptual model. We developed a calibration for the R watershed over a 6 month period of time in 2010. Results from the calibration are presented in figure 6.

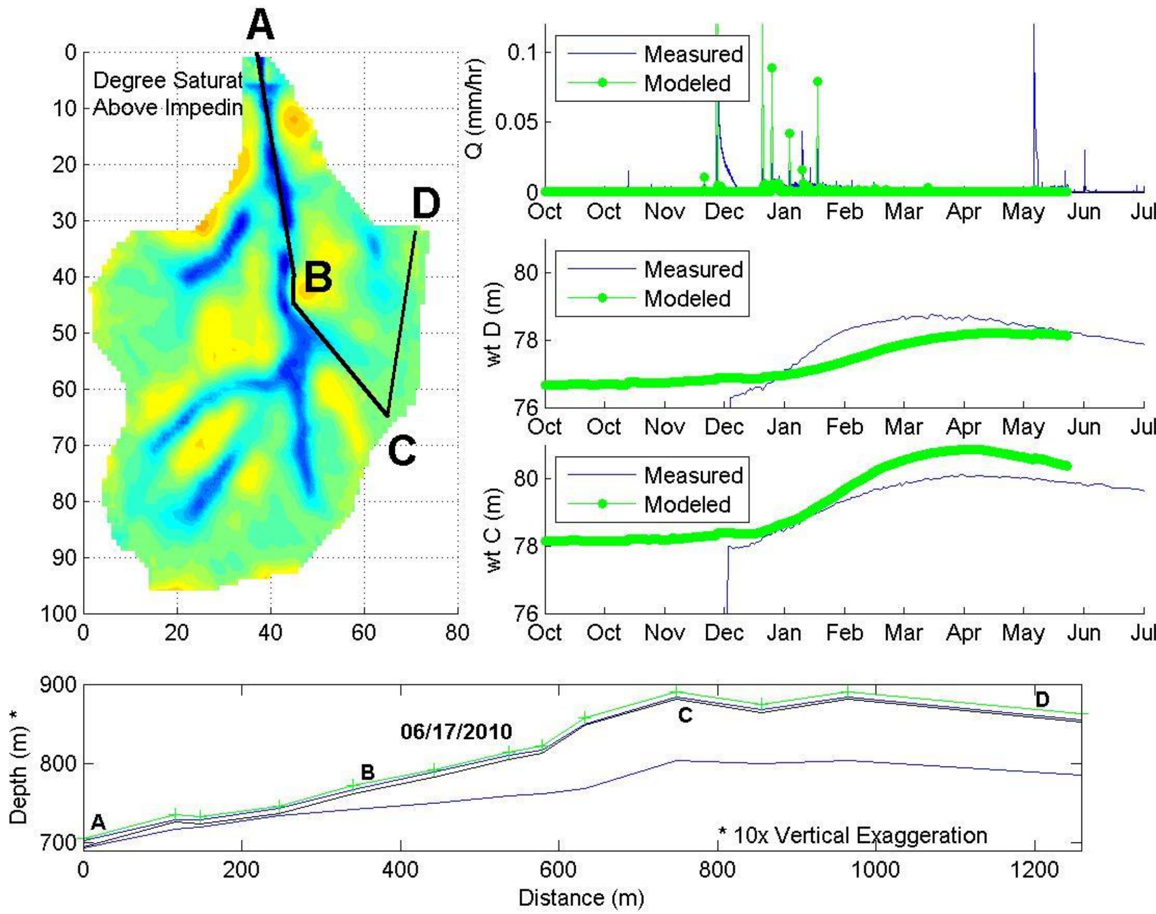

Figure 6. Calibrated results from the R watershed over a 6 month period in 2010. The map in the Upper right outlines the degree of saturation in the soils, where blue colors indicate wetter conditions and tend to develop and persist in hillslope hollows and near the channel. Greener colors represent dryer soils. Panel in the upper right is the measured vs modeled discharge hydrograph, collected in the stream near the point labeled A on the map. Below that are two plots of simulated versus observed well levels, at the points labeled D and C respectively. The figure across the bottom represents a cross sectional view of the catchment, from points DCBA on the map. The blue line represents the deeper groundwater, while the shallow groundwater is outlined (faintly, given the vertical scale) between the surface in Green and the depth of the soil, which we have assumed to be 1.5 meters.

The calibration at the R watershed appears to reasonably capture key dynamics, including the spatial distribution of soil and groundwater. The discharge simulations do pick up many of the peaks, and we note that it is difficult to capture them in greater detail because of uncertainties associated with the model and also with the measurements. From the measurement perspective, it is difficult to quantify how much water moves under and around the installed flumes.

Part 3. Verification at R B and C watersheds

Our initial verification strategy has been to run the 3 models using the calibrations from R, but at a different period of time. We elected to use the period from approximately 5/1/2010 to 5/1/2011. This period represents a time with relatively good data coverage in terms of stream discharge and meteorology. It also represents a challenging verification because it was a much wetter period of time, with significantly more observed runoff than the calibration period during 2010. We are still processing well level data from this period of time, and as such, those outputs related to observed water levels are not included in this report. Figures 7 and 8 represent some key mapped outputs for a time in early February 2011. These patterns indicate that the models for B and C are well setup. Results highlight that the spatial distribution of water in the soil and groundwater appears plausible, and responds to internal boundary conditions. This is particularly evident in Figure 6, center plate, where the central location with somewhat dryer soils corresponds to a sand soil (Wagram Sand). Similar figures representing R watershed have not been included.

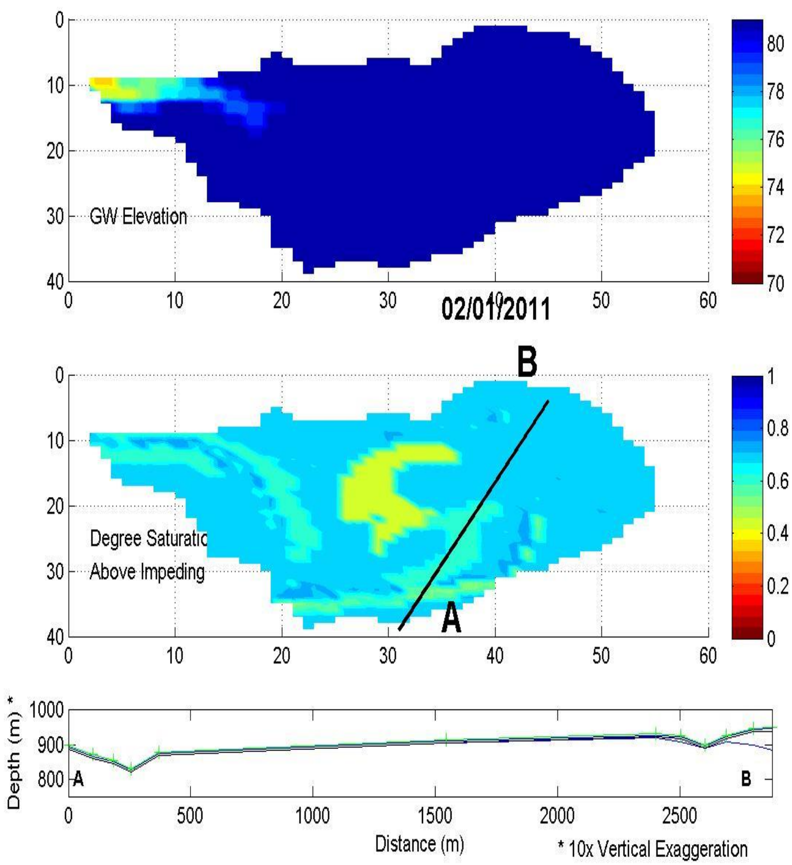

Figure 7. A snapshot of model results from C catchment. Upper plate represents the elevation (m above sea level) of the simulated groundwater. The middle plate represents the degree of saturation in the soil and the lower plate represents the water tables (in m above sea level, with 10 x vertical exaggeration) for the cross section labeled AB in the central plate

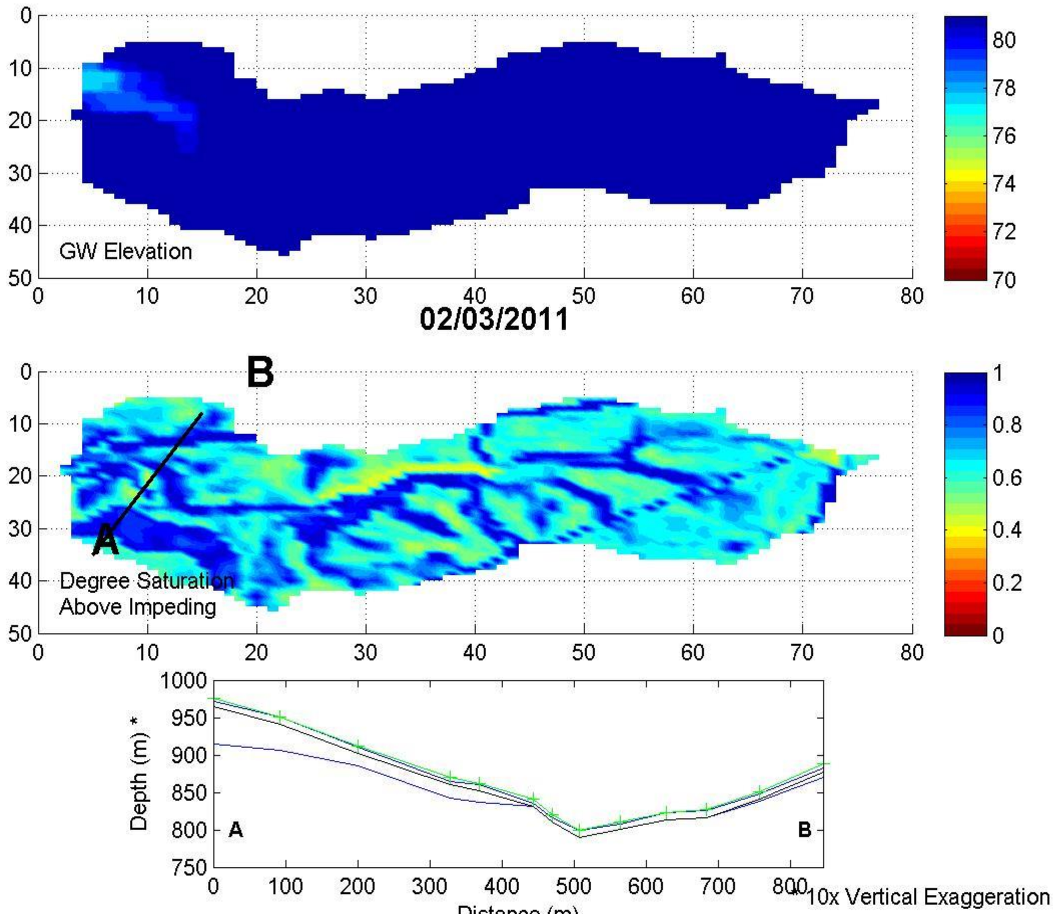

Figure 8. A snapshot of model results from B catchment. Upper plate represents the elevation (m above sea level) of the simulated groundwater. The middle plate represents the degree of saturation in the soil and the lower plate represents the water tables (in m above sea level, with 10 x vertical exaggeration) for the cross section labeled AB in the central plate.

Initial analysis of streamflow simulations (not shown) suggested that the direct transfer of the model parameters from the R watershed to B and C is not feasible: observed hydrographs are not well simulated. This result is not entirely surprising because of different meteorological conditions during the two periods of time and because of differences in potential undercatch in the observational flumes at each of the three sites.

To more fully explore how the current model structure performs relative to wetter verification period, we developed a set of monte carlo analyses, varying some key model parameters to evaluate the degree to which simple changes to parameters, rather than changes to the structure of the model itself, might improve model performance. Refer to Figures 9 and 10 for a representation of these monte carlo results. The development of these results was based on the Monte Carlo Analysis Toolkit (MCAT) (Wagener et al., 2006).

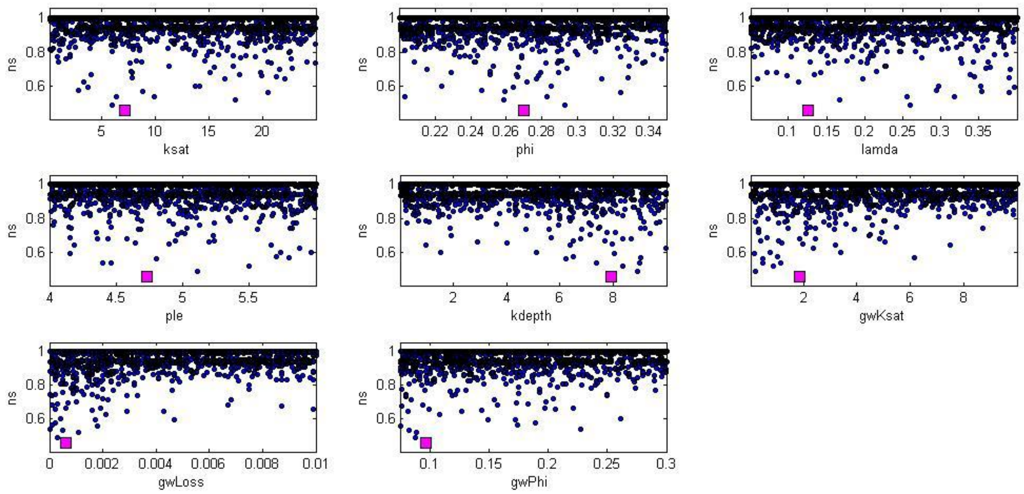

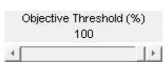

Figure 9. A figure outlining the monte carlo runs for watershed C. Each plot represents a model parameter (horizontal axes) and a version of the Nash-Sutcliffe efficiency quantifying, as single value, the degree to which any particular model (meaning set of parameters) captured the observed hydrograph. The best parameter set is highlighted as a red box.

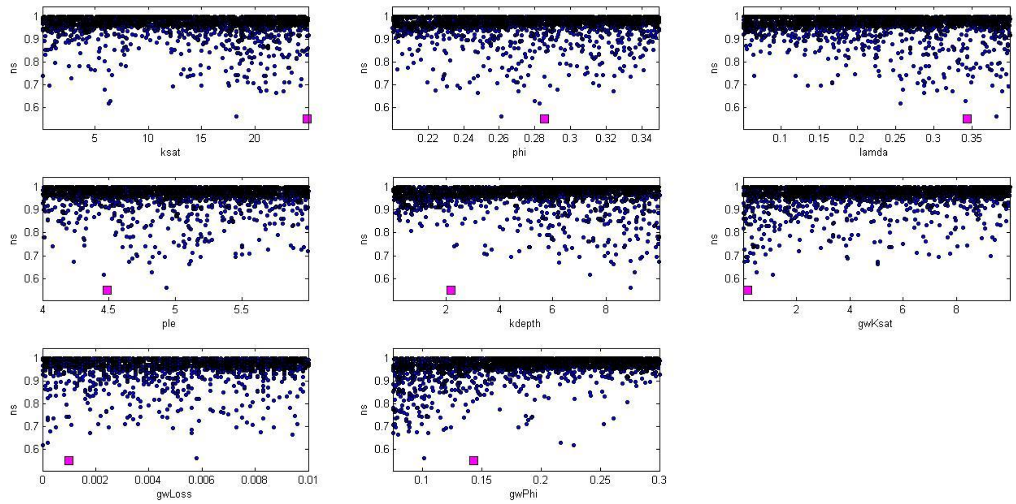

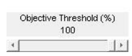

Figure 10. A figure outlining the monte carlo runs for watershed B. Each plot represents a model parameter (horizontal axes) and a version of the Nash-Sutcliffe efficiency quantifying, as single value, the degree to which any particular model (meaning set of parameters) captured the observed hydrograph. The best parameter set is highlighted as a red box.

The scatter plots (Figures 9 and 10) provide a quick look at key parameters, and the degree of 'identifiability' (Wagener et al., 2006) of the model. Like most hydrological models, it is not highly identifiable, meaning similar fits to the hydrograph can be found across the range of feasible parameter sets. This range is generally translated into confidence bands or uncertainty intervals about the prediction.

A set of confidence limits, as defined by Wagener et al. (2006), is included for B and C during the verification period in Figure 11. In this figure, the blue dots represent the measured stream discharge (m3/s) and the two black lines represent confidences intervals based on the monte carlo results. Note that in both figures, the lower confidence limit falls to a value of 0 early in the simulation. The uncertainty interval is rather large, and does not fully include the observations, in particular for B watershed (bottom). This deviation is larger than is often found in hydrological models, but given associated uncertainty with the observations themselves; we view them as acceptable at this point in the modeling work. Ongoing refinements to the model, including methods to include the updated conceptual model and more fully evaluated observed datasets will likely improve simulated stream flow over the project timeframe.

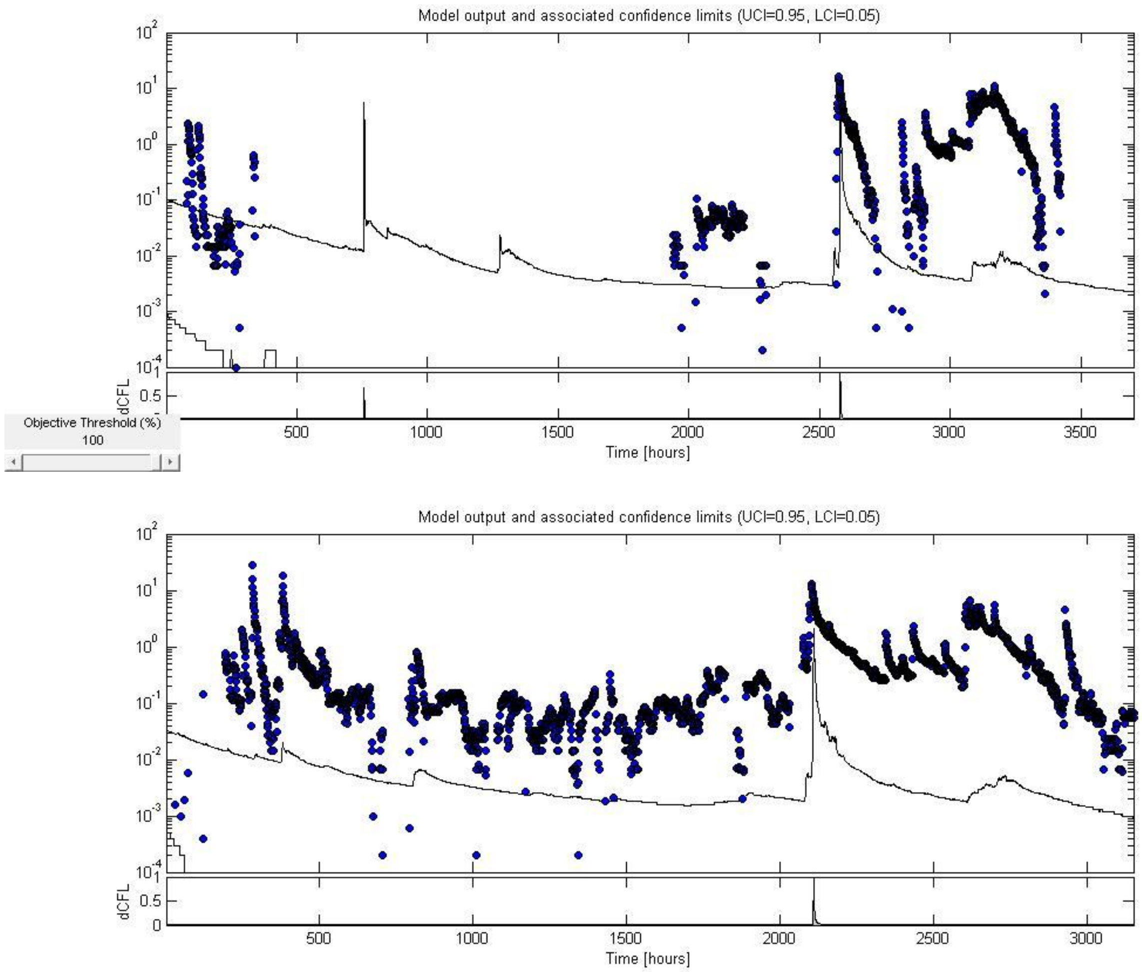

Figure 11. Figure captures both simulated (black line) and observed (blue dots) stream flow, in m3s, for the C watershed (top) and B watershed (bottom). Note that these are log linear plots to highlight both high and low flows.The small panels, labeled dCFL represent the degree of similarity between the two time series (observed and simulated) in linear space.

Conclusions

The key water balance components for the SRS subwatersheds R, B, and C have be developed within the distributed modeling framework. The model incorporates key datasets, shows needed sensitivity to landuse and management, and appears to work acceptably well, given the mid-project date. We anticipate further refinements as new data becomes available and as we more fully evaluate those observations.

References

Federer, C.A., Vorosmarty, C. and Fekete, B. (1996), Intercomparison of methods for calculating potential evaporation in regional and global water balance models. Water Resources Research 32(7): doi: 10.1029/96WR00801. issn: 0043-1397.

Shuttleworth, W.J. (1993), Evaporation. In: Maidment, D.R. (Ed.),Handbook of Hydrology. McGraw-Hill, New York, pp. 4.1–4.53.

Shuttleworth, W.J., Wallace, J.S. (1985), Evaporation from sparse crops – an energy combination theory. Quart. J. Royal Meteorol.Soc. 111, 839–855.

Shuttleworth, W.J., Gurney, R.J. (1990), The theoretical relationship between foliage temperature and canopy resistance in sparse crops. Quart. J. Royal Meteorol. Soc. 116, 497–519.

Vaché, K. B., and J. J. McDonnell (2006), A process-based rejectionist framework for evaluating catchment runoff model structure,*Water Resour. Res.*, **42**, W02409, doi:10.1029/2005WR004247.

Vaché, K. B., C.R. Jackson, M.M. Bitew, J. Blake, J.J. McDonnell, and N. Griffiths. 2013.Potential impacts of intensive cellulosic biofuel production on water quality and quantity in theUpper Coast Plain, US. Abstract H11B-1158 presented at 2013 Fall Meeting, AGU, SanFrancisco, Calif., 9-13 Dec.

Wagener, T., Boyle, D. P., Lees, M. J., Wheater, H. S., Gupta, H. V., and Sorooshian, S. (2001), A framework for development and application of hydrological models (2002) Hydrol. Earth Syst. Sci., 5, 13-26, doi:10.5194/hess-5-13-2001.

Wigmosta, M. S., L. W. Vail, and D. P. Lettenmaier (1994), A distributed hydrology-vegetation model for complex terrain, Water Resources Research, 30(6), 1665-1679.